

We are IntechOpen, the world's leading publisher of Open Access books Built by scientists, for scientists

6,900

Open access books available

186,000

International authors and editors

200M

Downloads

Our authors are among the

154

Countries delivered to

TOP 1%

most cited scientists

12.2%

Contributors from top 500 universities



WEB OF SCIENCE™

Selection of our books indexed in the Book Citation Index
in Web of Science™ Core Collection (BKCI)

Interested in publishing with us?
Contact book.department@intechopen.com

Numbers displayed above are based on latest data collected.
For more information visit www.intechopen.com



Piezoelectric Energy Harvesting

Hiroshi Maiwa

Additional information is available at the end of the chapter

<http://dx.doi.org/10.5772/64162>

Abstract

The piezoelectric material selection and the circuit design in vibrational energy harvesting are discussed. The performances of the energy-harvesting unimorph devices that captured frequencies of 60 Hz by using piezoelectric PZT-based and BT-based ceramics were evaluated. Output voltages and power from the devices depend on the amplitude and the frequency of the oscillations, and depend on the load resistance. Generally, PZT-based ceramics are superior for piezoelectric energy-harvesting applications. The figures of merit of the materials are discussed in order to provide the guidelines of the piezoelectric material selections. Piezoelectric voltage coefficient, g_{31} , is considered to be good parameter to predict the maximum voltages. On the other hand, $d_{31}g_{31}/\tan\delta$, $k_{31}^2Q_m$ and $d_{31}g_{31}$ are close to the behavior of the maximum power. Combination of the piezoelectric unimorph and power management circuit produced the constant voltage output, which would be used as the power sources.

Keywords: energy harvesting, piezoelectricity, lead-free, power management circuit

1. Introduction

Energy harvesting (EH) is the process of capturing small amounts of energy from external natural energy sources, accumulating and storing them for later use. In many cases, EH devices convert ambient energy into electrical energy. By combining suitable electronics, EH devices can be used for creating a self-sufficient energy supply system. The merits of the system include the replacement or supplement of the batteries and the minimization of the associated maintenance expenditure, and the replacement of the power supply cables. Major application target of EH is for independent sensor networks [1]. The aspect of the sensor network is illustrated in **Figure 1**. The sensor network is consisted of the wireless sensors placed on various places, such as human body, vehicles, and buildings, in order to monitor the physical or environmental

conditions, such as temperature, humidity, sound, pressure, etc. The data are gathered from the sensor nodes to data center through the gateway sensor node. The compositions of the sensor node are illustrated in the upper right side of **Figure 1**. Sensor node is consisted with a radio transceiver with an antenna, a microcontroller, an electronic circuit for interfacing with the sensors, and an energy source. EH is attracting an attention for the embedded energy source of sensor nodes and is considered to be one of the key technologies of Internet of things (IoT). In the last decade, the field of EH has increasingly become important as illustrated in the rising numbers of publications in **Figure 2**.

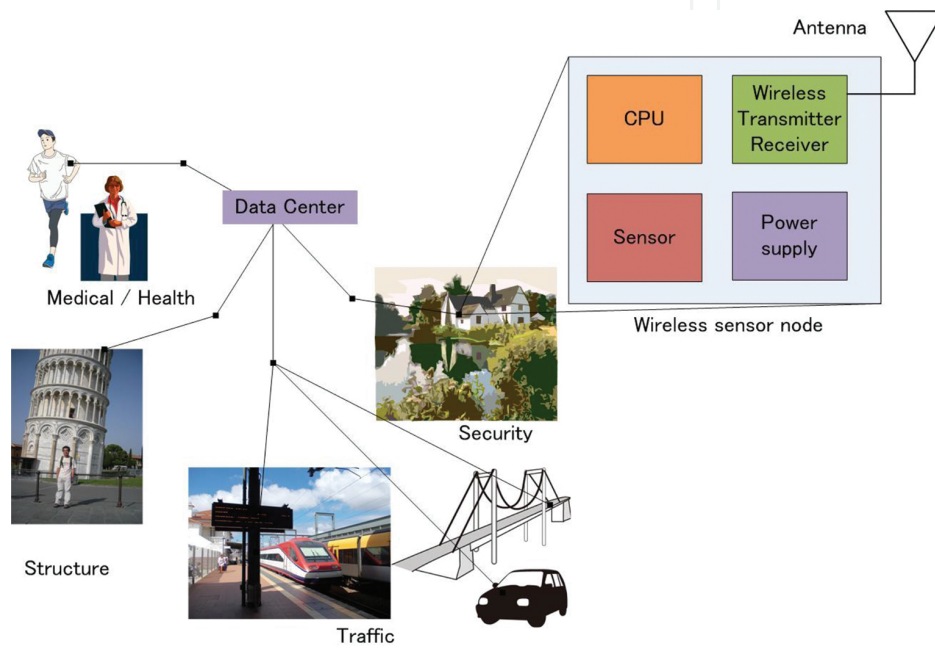


Figure 1. The architecture of the sensor network. The configuration of sensor network consisting of sensors placed on various places. The compositions of the sensor node are illustrated in the upper right side.

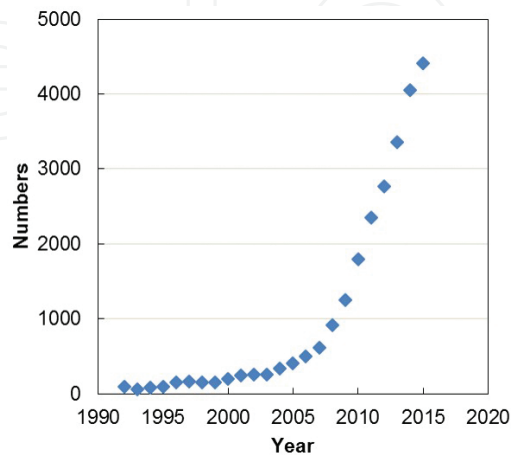


Figure 2. Year-to-year comparison of the numbers of papers on energy harvesting, 1958–2015.

The available energy from the environment includes solar power, thermal energy, wind energy, salinity gradients, and kinetic energy. Solar energy has the capability of providing large power density outdoors; however, it is not easy to capture the adequate solar energy in indoor environment. Mechanical vibration is the most attractive alternative [1, 2]. Vibration-electrical energy harvesting using piezoelectric effects has been explored for possible use in sensor network modules [1–11]. In order to harvest energy from the environment, it is necessary to capture vibrations with frequencies less than 200 Hz, because such frequencies are dominant in normal life and in vehicles, as shown in **Table 1** [12, 13].

Origin of the vibrations	Acceleration (m^2/s)	Frequency (Hz)
3-Axis machine	10	70
Cooking mixer	6.4	121
Clothes dryer	3.5	121
Electric oven (small size)	2.25	121
Air exhaust in buildings	0.2-1.5	60
Wood deck with traffic	1.3	385
Windows facing busy street	0.7	100
Note PC loading CD	0.6	75
Washing machine	0.5	109
Refrigerator	0.1	241

Table 1. Acceleration and frequency of the vibration sources in the environment [13].

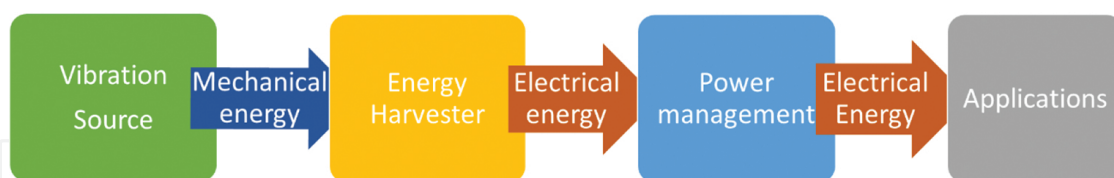


Figure 3. Typical components of the vibrational energy-harvesting systems. Mechanical energy is converted to electrical energy by energy harvester and is adjusted the output by the power management circuit.

Considering the application to the power source, appropriate power management circuit design to adjust to the requirement of the application devices. The block diagram of the vibrational energy-harvesting systems is illustrated in **Figure 3**. Energy harvester is vibrated by the excitation force of the vibration source, then the mechanical energy is converted to electrical energy by piezoelectrics in energy harvester. The generated electrical energy is consumed in the application circuits; finally, the optimum control of an electrical output in accordance with a load condition of the applications is required. Therefore, the power management circuit plays an important role in the system. The block diagram of the power management circuit is shown in **Figure 4**. Since the voltage and current of the electricity

generated by the piezoelectric energy harvester are alternating, diode rectifier has required to produce direct current (DC) power supply. And the electricity from the piezoelectric power generator is large amplitude and frequency fluctuations; therefore, regulation circuit is required. DC-DC convertor is controlled by regulation circuit to adjust the requirement of the applications. The output voltage from the piezoelectric generator, the output voltage after rectification, and the controlled voltage output are shown in **Figure 5(a–c)**, respectively. Alternating voltage having a waveform of almost positive negative symmetry is generated by piezoelectric generator. By full wave rectifying circuit, the generated voltage was converted to one of constant polarity (positive or negative). Smoothing capacitor or filter is required to produce the steady direct voltage. The regulated circuit including capacitor and DC-DC convertor produced constant voltage output. In order to enhance the performance of the energy-harvesting circuit, a nonlinear processing technique “synchronized switch harvesting on inductor” (SSHI) [5], or active full-wave rectifier by using CMOS (complementary metal oxide semiconductor) technology [14], and power conditioning circuit with maximum power point tracking (MMPT) have been proposed [15].

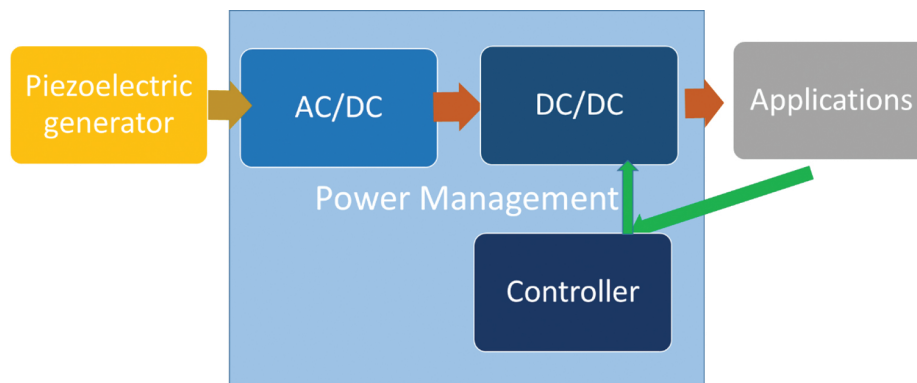


Figure 4. Block diagram of the power management circuit in the energy-harvesting systems. The power management circuit is composed of the AC-DC converter, DC-DC convertor, and the controller to adjust the requirement of the applications.

In order to obtain energy harvesters with high performances, material selections are important problems. From the view point, figures of merit of the materials have been discussed thus far. Priya has provided dimensionless figures of merit (DFOM) for a 3–1 mode transducer under on-resonance and off-resonance conditions, as follows.

$$\text{DFOM} = (k_{31}^2 Q_m / s_{11}^E)_{\text{on-resonance}}$$

$$\text{DFOM} = (d_{31} g_{31} / \tan \delta)_{\text{off-resonance}}$$

Here, k_{31}^2 , Q_m , s_{11}^E , d_{31} , g_{31} , and $\tan \delta$ are the electromechanical coupling factor, mechanical quality factor, piezoelectric strain coefficient, piezoelectric voltage coefficient, and loss tangent, respectively [9].

Takeda et al. have suggested that power output from vibration-based generators should be expressed as linear functions of the term composed of electromechanical coupling coefficients k_{sys}^2 and the mechanical quality factor Q_m^* of the generator, which enables output estimation

using material constants k_{31}^2 and Q_m [10]. However, the aspects of the ambient vibration and required electrical characteristics as converters are diverse, and obtaining a full understanding of the appropriate material properties for various applications is still challenging.

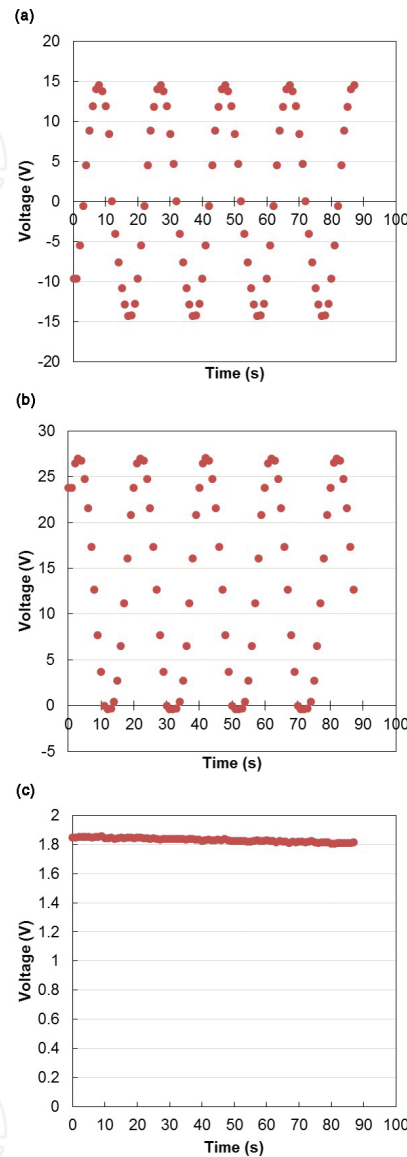


Figure 5. The output voltages (a) from the piezoelectric generator (b) after rectification with a full-wave rectifier using four diodes and (c) controlled by using power management circuit.

In our previous study [16, 17] the unimorphs—cantilevers with an active piezoelectric layer and an inactive elastic layer—were fabricated, and, preliminary results on the performance were reported. Although EH devices fabricated by using thin film piezoelectrics are advantageous in the miniaturization and mass-productivity, EH devices fabricated by using bulk ceramics are superior in power output. Moreover, in the case of the unimorph EH devices by using bulk ceramics, material selections are easy by just replacing the ceramics. While, in the case of EH devices by using thin films, film deposition process is depending on the materials,

comparative study of materials is relatively difficult. From the perspective of minimizing the environmental load by avoiding the use of lead-containing materials, consideration of lead-free piezoelectric materials is valuable for energy-harvesting devices [13]. Therefore, in addition to PZT-based ceramics, barium titanate (BT)-based ceramics was evaluated for piezoelectric materials in this chapter. The performance of piezoelectric energy-harvesting devices that captured frequencies of 60 Hz for PZT-based and BT-based ceramics was evaluated and the figures of merit of the materials have been discussed in order to provide the guidelines of the piezoelectric material selections. The results using power management circuit are included for evaluating the performance as the power source.

2. Experimental

The commercial piezoelectric bimorph is used for basic operations in the power management circuit. And the piezoelectric unimorph were fabricated by remodeling the commercial bimorphs. The experimental setup for measuring the unimorph generator is shown in **Figure 6**. Details were described in our previous study [16]. Commercial bimorph was produced by using a patterned fiber-reinforced plastic (FRP) plate ($105 \text{ mm} \times 10 \text{ mm} \times 1.6 \text{ mm}$) that was used as the base beam. Piezoelectric ceramics was adhered to both the side of the beam. The unimorph structure was fabricated by removing the piezoelectric ceramics from both the side and adhering PZT- or BT-based ceramics ($10 \text{ mm} \times 18 \times 0.5 \text{ mm}$) to one side of the FRP beam. The unimorph was attached to the vibration generator and oscillated with various frequencies and accelerations. And the characteristic frequency of the beam was 57

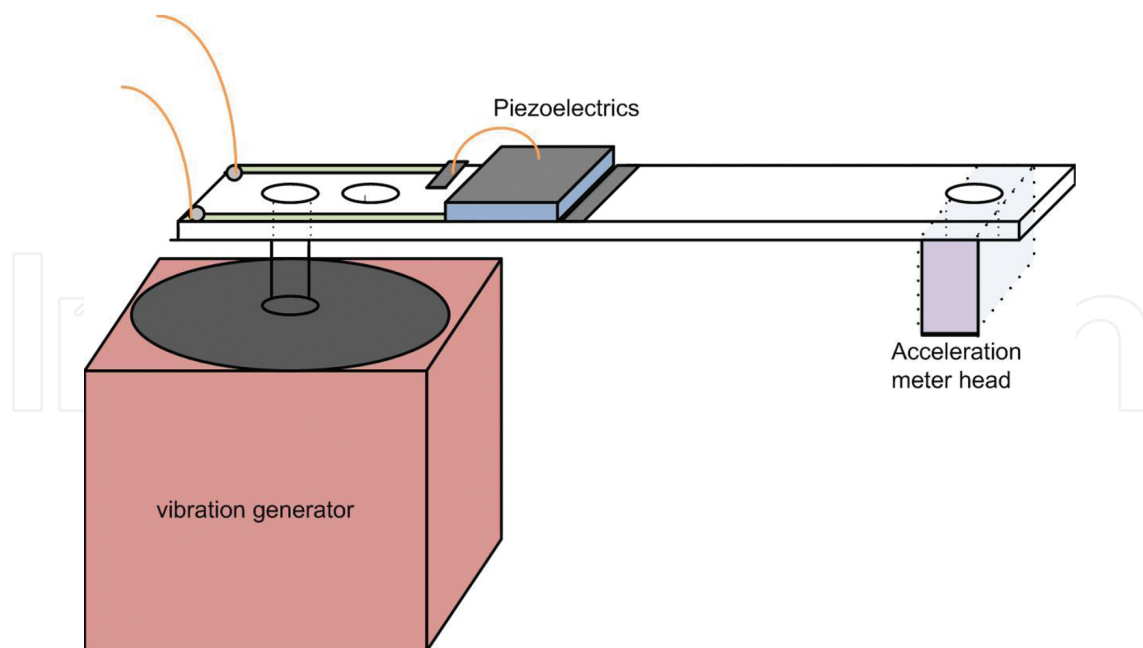


Figure 6. The experimental setup for measuring the unimorph generator. The unimorph constructed by the piezoelectric ceramics and FRP beam was attached to the vibration generator and oscillated with various frequencies and accelerations. The displacements and accelerations of the unimorph were monitored by the acceleration sensor attached to the other end during measurement [16].

Hz. An acceleration sensor was attached to the other end, and the displacements of the unimorph were monitored during measurement. The beam vibrated with the tip as a node at 60 Hz.

In the case of the unimorphs, commercial bulk PZT ceramic disks were used. The PZT-based ceramic disks were hard PZT ceramics with T_c of 325°C, soft PZT ceramics with T_c of 145, 190, or 330°C (hereafter PZTh325, PZTs145, PZTs190, or PZTs330, hereafter, respectively, NEC Tokin) of 0.5 mm thickness were used [15]. As lead-free ceramics, nondoped BaTiO₃ (BT) ceramics, manganese-doped BaTiO₃ (BT-Mn), and (Ba_{0.85}Ca_{0.15})(Ti_{0.95}Zr_{0.05})O₃ (BCCZ5) sintered at 1400°C, 1300°C, and 1350°C, respectively, were used. The dielectric and piezoelectric properties of these ceramics are shown in **Table 2** and were reported in detail in our previous study [16, 18].

Samples	Dielectric constant	Q_m	k_{31}	g_{31} (mVm/N)	d_{33} (pC/N)	Maximum voltage (V)	Maximum power (μW)
PZTh325	1190	461	35.3	11.8	347	19.6	19.2
PZTs145	4940	66.7	34.4	6.2	507	18.4	72.2
PZTs190	3578	64.8	32.8	7.1	445	38	351
PZTs330	1509	71.4	36.3	11.9	370	56	307
BT	3173	51.9	18.8	4.1	158	2.6	0.8
BT-Mn	3635	95.3	11.7	2.2	85	11	24.5
BCCZ5	1867	66.3	12.4	2.6	63	9.8	17

Table 2. Voltage, power, and material parameters of the piezoelectric samples [16].

In order to evaluate the performance as an energy source, a piezoelectric energy-harvesting power supply integrated circuit (LTC3588-1, Linear Technology Corp.) that integrates a low-loss full-wave bridge rectifier with a high efficiency buck converter was employed [19]. The bimorphs were oscillated for 45 sec. In this power supply circuit, V_{in} voltage rectified by a full-wave bridge rectifier that rectifies AC input from piezoelectric elements, and P_{good} power good output signal signifying that the output voltage produced by the converter in the power supply exceeding 92% of the programmed output voltage of 3.6 V, were outputted.

3. Results and discussion

The frequency dependence of the V_{charge} from the piezoelectric unimorph is shown in **Figure 7**. The V_{charge} shows the maximum at 57 Hz, indicating that the maximum displacement of the bimorph provides the largest voltage output. The output voltages across the various load resistors were measured. **Figure 8** shows the load voltage delivered to load resistance by oscillating the unimorph with a relative displacement of 0.2, 0.4, and 0.8 mm and a frequency of 60 Hz. It is found that the voltage increases proportionally to the relative displacement. From the voltage, the output electric powers, P , at the load resistance were calculated using

$P=1/2(V^2/R)$ equation. The results are shown in **Figure 9**. It is noted that the electric powers varied with the load resistance. In all samples, the power increases with increasing resistance and showed that their peak power decreases with increasing resistance. The resistance that yielded maximum power varied with the samples, this resistance roughly correspond to the resistance of the samples. These results were very close to our previous results; however, the hard PZT ceramics yielded higher output voltage but smaller power in this study. The reason for this phenomenon is not yet clear. In the case of the hard PZT, the electrical damping may be larger [13]. Unimorph that used PZT with higher T_c generates larger voltage and power. Concerning generators that used BT ceramics, Mn-doping was effective. Mn-addition raises Q_m in BT ceramics, and PZT with higher T_c exhibits higher Q_m . The results of this study suggest that hard piezoelectric properties would be favorable for a piezoelectric generator. The relation between maximum voltage or power and the materials' parameter from the unimorph using various ceramics is shown in **Figures 10** and **11**, respectively. For maximum voltage, g_{31} is considered to be good parameter. For maximum power, $d_{31}g_{31}/\tan\delta$, $k_{31}^2Q_m$ and $d_{31}g_{31}$ are close to the behavior of the maximum power; however, hard PZT ceramics yielded smaller power, compared with the expected values estimated from the material parameters.

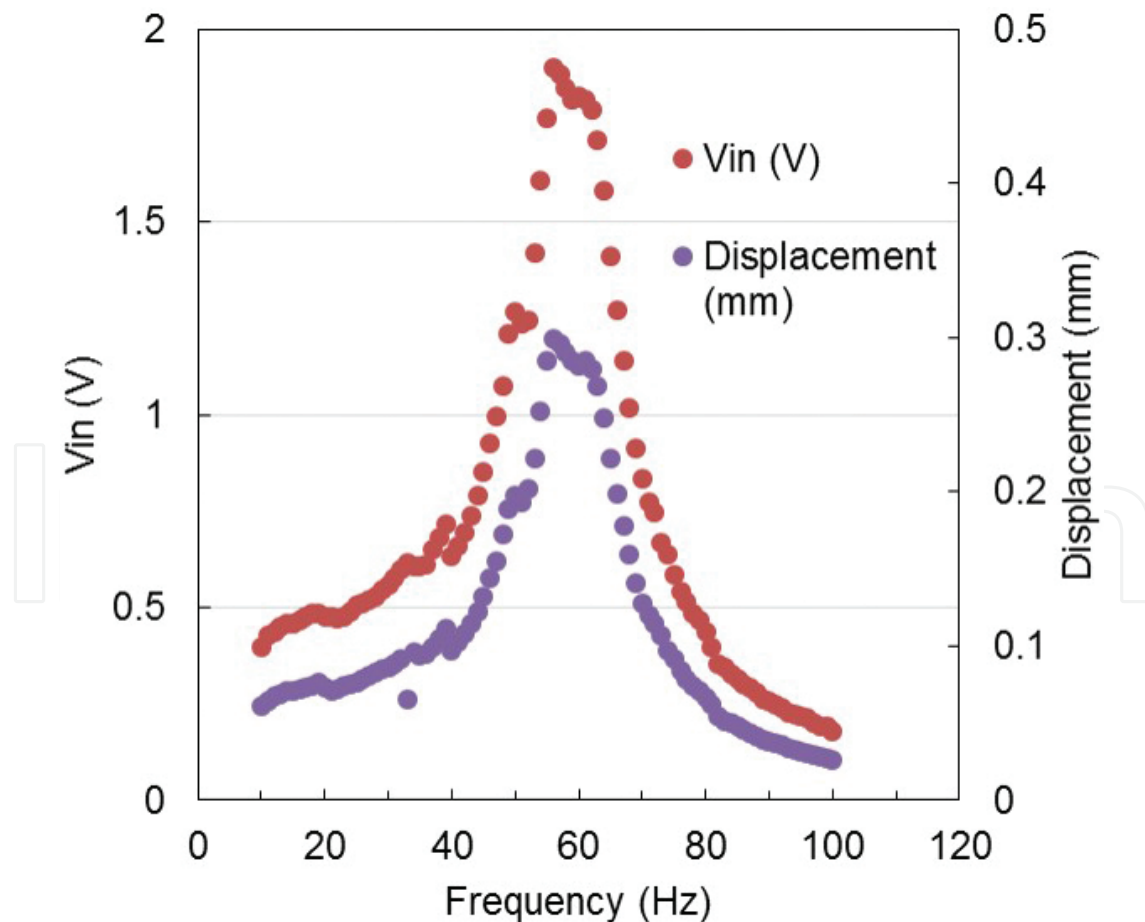


Figure 7. Frequency dependence of V_{charge} voltages from the unimorph generator.

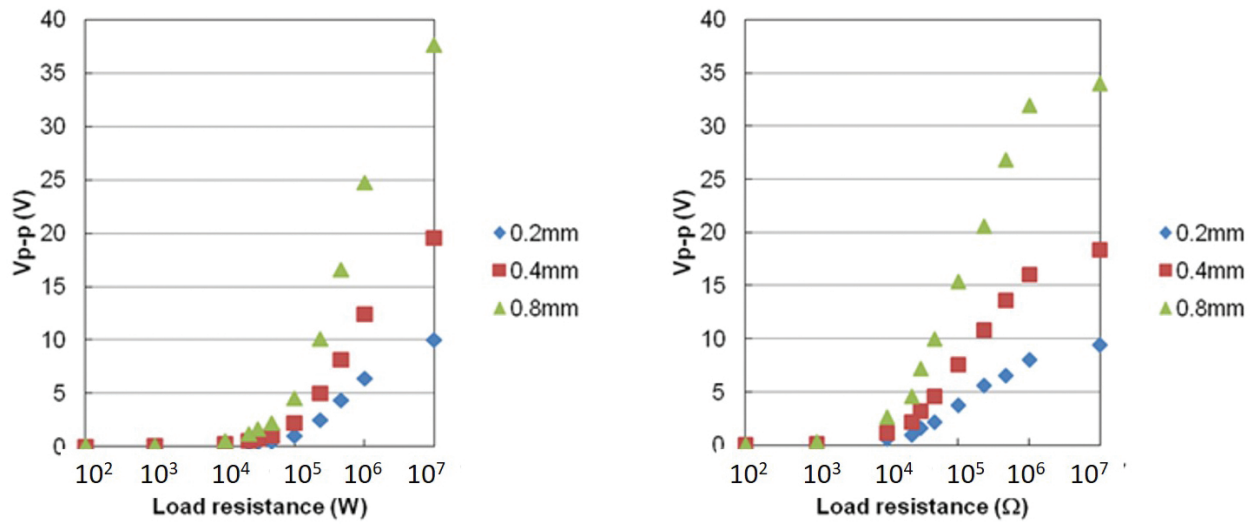


Figure 8. Load resistance dependence of the output voltage from the unimorph using (a) PZTh325 and (b) PZTs140 ceramics.

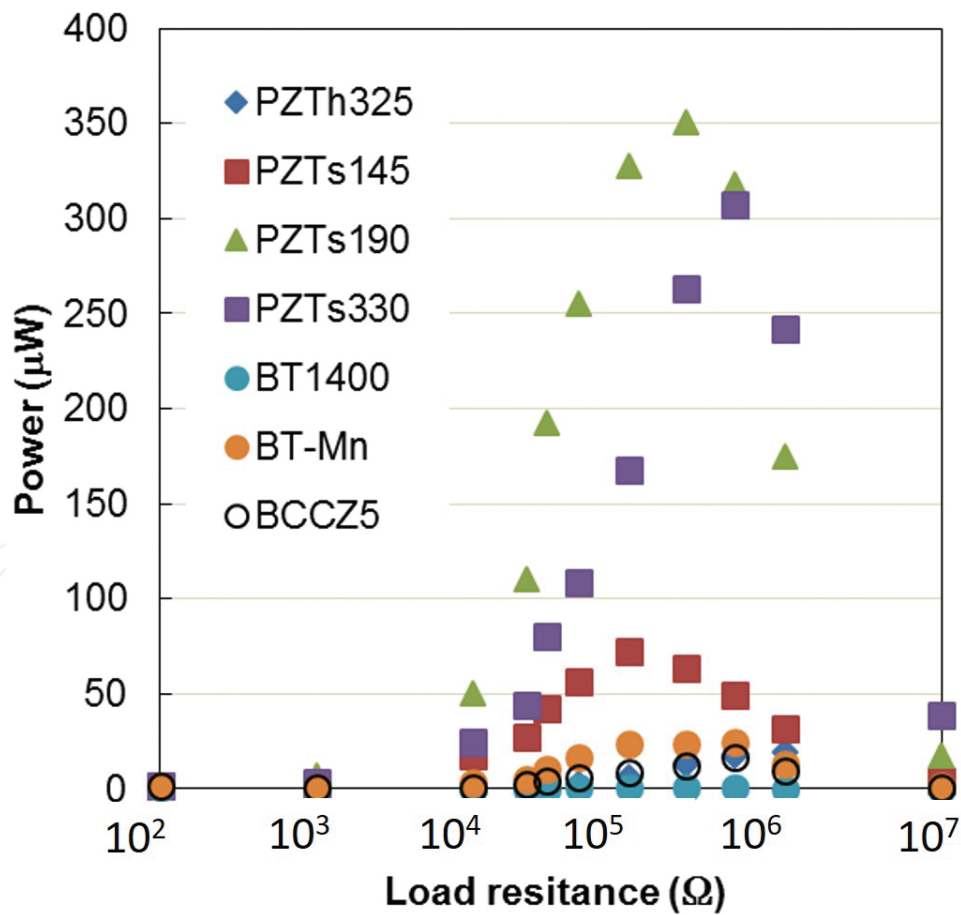


Figure 9. Load resistance dependence of the output power from the unimorph using various ceramics. The output electric powers, P , at the load resistance, R , were calculated using $P=1/2(V^2/R)$ equation from the output voltage, V .

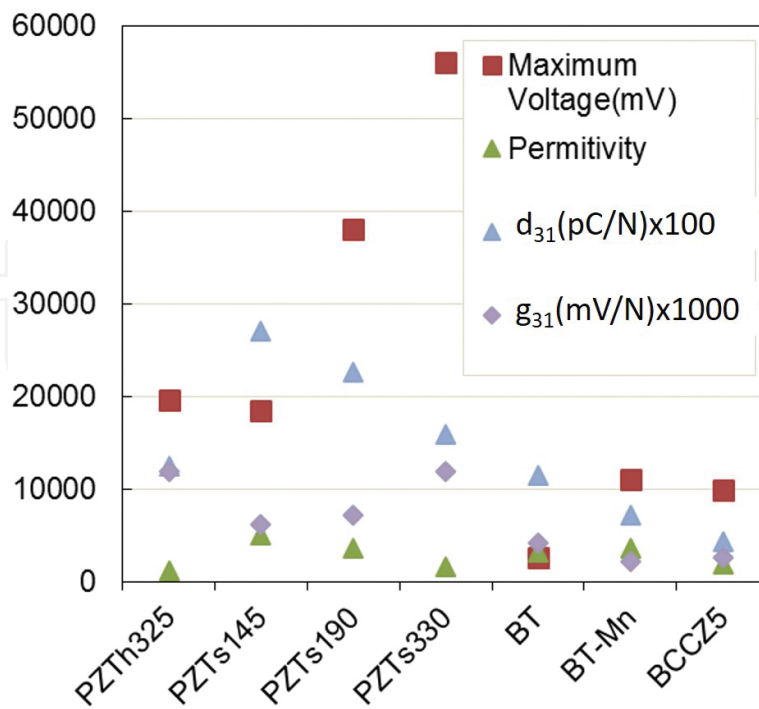


Figure 10. The relation between maximum voltage and various material parameters.

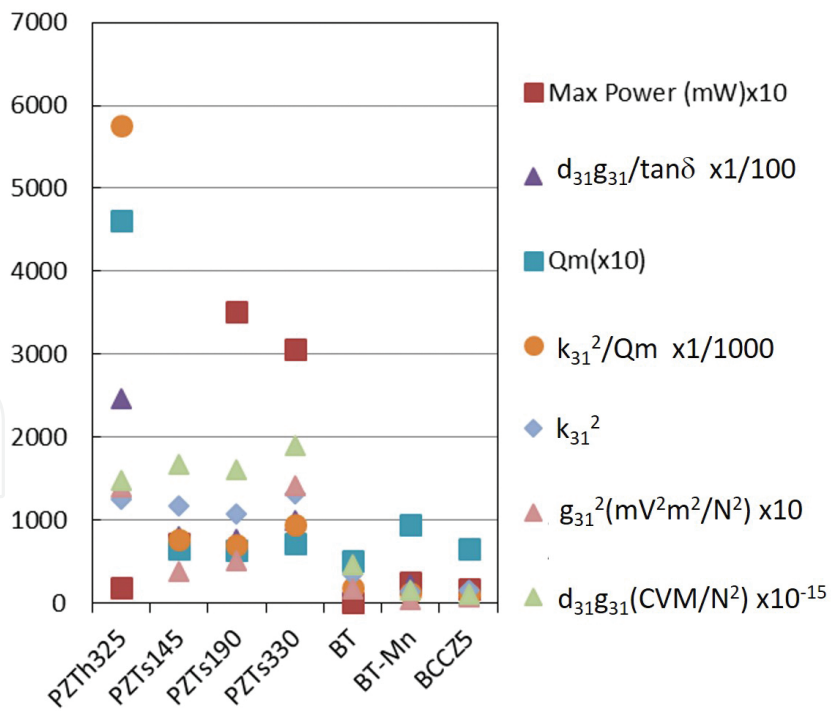


Figure 11. The relation between maximum power and various material parameters.

The charging voltage (V_{charge}), oscillation signal (vibration), and P_{good} were measured by oscillating the unimorphs consisted with PZTs330 and BT-Mn at 60 Hz for 45 sec. The results

are shown in **Figure 12(a and b)**. The V_{charge} keeps constant voltage during oscillation, and the voltage damped shortly after the quitting the oscillation. Time constant of the damped oscillation was 3.4 s for both measurements. Considering that the capacitance (C) of the charging capacitor is 22 μF , the damping behavior is reasonable. P_{good} keeps constant during oscillation and a few seconds after quitting the oscillation for both measurements, showing the unimorph EH generators used in this study have the capability of the power sources. The stored energy is calculated by using the $(1/2)CV_{\text{in}}^2$ equation. The stored power is calculated by dividing the stored energy by an oscillation time of 45 sec. The maximum output voltage and power across the load resistance, stored power, and energy in the capacitor and P_{good} time are summarized in **Table 3**. The relations among voltage, power, and energy are roughly related; however, the relations are not so simple with careful evaluation. For example, maximum powers are dependent on the load resistance, while the stored power and energy are more closely related to the output voltage. The operation of the power supply integrated circuit might require voltage to the high impedance input from the piezoelectric generators.

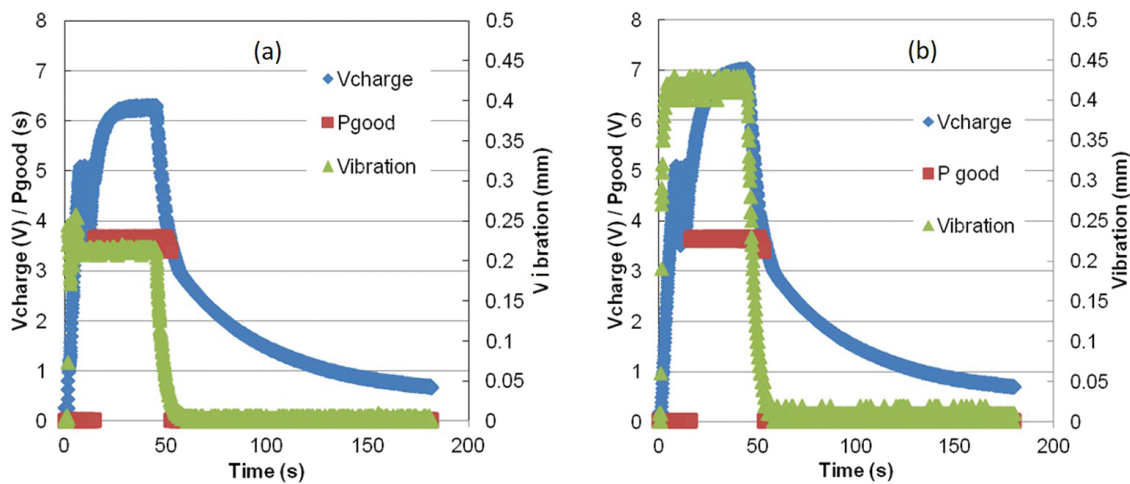


Figure 12. V_{Charge} oscillation signal (vibration), and P_{good} measured by oscillating the unimorphs consisted with (a) PZTs330 and (b) BT-Mn at 60 Hz for 45 sec.

Samples	Maximum voltage (V)	Maximum power (μW)	Energy (μJ)	P_{good} (s)
PZTh325	19.6	19.2	233	0
PZTs145	18.4	72.2	423	38
PZTs190	38	351	2753	56
PZTs330	56	307	3493	55
BT	2.6	0.8	16	0
BT-Mn	11	24.5	194	0
BCCZ5	9.8	17	135	0

Table 3. Performances of the piezoelectric generator with piezoelectric ceramics [16].

4. Conclusion

The performance of piezoelectric energy-harvesting devices fabricated from the base FRP beam and PZT-based and BT-based ceramics that captured frequencies of 60 Hz was evaluated. The output voltage from the generator is proportional to the displacement of the piezoelectric ceramics. And the output voltages from the bimorph and unimorph generator varied with the applied frequencies. The output voltage increased with the load resistance, on the other hand, the output power showed the maximum at around the load resistance with the impedance of the piezoelectric generators. And the figures of merit of the materials have been discussed in order to provide the guidelines of the piezoelectric material selections. Piezoelectric voltage coefficient, g_{31} , is considered to be good parameter to predict the maximum voltages. On the other hand, $d_{31}g_{31}/\tan\delta$, $k_{31}^2Q_m$, and $d_{31}g_{31}$ are close to the behavior of the maximum power, these material parameters are suitable to evaluate the EH performance. The performance of the power management circuit was evaluated. The constant voltage output was confirmed during oscillations of the piezoelectric generators, showing the systems used in this study have the capability of the power sources. As a conclusion, the results of this work suggested that the piezoelectric material selection and the circuit design are important problems to implement piezoelectric generator to the various applications.

Acknowledgements

This study was supported in part by a grant from JSAP KAKENHI Grant Number 26420684, and a Green Network of Excellence (GRENE) project grant from the Ministry of Education, Culture, Sports, Science, and Technology, Japan. And part of figures and tables are reprinted with permission from Taylor and Francis.

Author details

Hiroshi Maiwa

Address all correspondence to: maiwa@mate.shonan-it.ac.jp

Department of Materials and Human Environmental Sciences, Shonan Institute of Technology, Tsujido-Nishikaigan, Fujisawa, Japan

References

- [1] Priya S and Inman DJ, editors. Energy Harvesting Technologies, Springer Science + Business Media; 2009, New York, USA. DOI: 10.1007/978-0-387-76464-1.

- [2] Roundy S: On the effectiveness of vibration-based energy harvesting. *Journal of Intelligent Material Systems and Structures*. 2005;16:809–823. DOI: 10.1177/1045389X05054042.
- [3] Poulin G, Sarraute E, and Costa F: Generation of electrical energy for portable devices: comparative study of an electromagnetic and a piezoelectric system. *Sensors and Actuators* 2004;A116:461–471. DOI: 10.1016/j.sna.2004.05.013.
- [4] Beeby SP, Tudor MJ, and White NM: Energy harvesting vibration sources for micro-systems applications. *Measurement Science and Technology* 2006;17:R175-R195. DOI: 10.1088/0957-0233/17/12/R01.
- [5] Guyomar D, Jayet Y, Petit L, Lefeuvre E, Monnier T, Richard C, and Lallart M: Synchronized switch harvesting applied to self-powered smart systems: piezoactive micro generators for autonomous wireless transmitters. *Sensors and Actuators* 2007;A138:151–160. DOI: 10.1016/j.sna.2007.04.009.
- [6] Erturk A and Inman DJ: An experimentally validated bimorph cantilever model for piezoelectric energy harvesting from base excitations. *Smart Materials and Structures* 2009;18:025009. DOI: 10.1088/0964-1726/18/2/025009.
- [7] Kim H, Priya S, Stephanou H, and Uchino K: Consideration of impedance matching techniques for efficient piezoelectric energy harvesting. *IEEE Transactions on Ultrasonics, Ferroelectrics, and Frequency Control*. 2007;54:1851–1859. DOI: 10.1109/TUFFC.2007.469.
- [8] Wang QM, Du XH, Xu B, and Cross LE: Electromechanical coupling and output efficiency of piezoelectric bending actuators. *IEEE Transactions on Ultrasonics, Ferroelectrics, and Frequency Control*. 1999;46:638–648. DOI: 10.1109/58.764850.
- [9] Islam RA and Priya S. Realization of high-energy density polycrystalline piezoelectric ceramics. *Applied Physics Letters* 2006;88:0329031. DOI: 10.1063/1.2166201.
- [10] Priya S: Criterion for material selection in design of bulk piezoelectric energy harvesters. *IEEE Transactions on Ultrasonics, Ferroelectrics, and Frequency Control* 2010;57:2610–2612. DOI: 10.1109/TUFFC.2010.1734.
- [11] Takeda H, Mihara K, Yoshimura T, Hoshina T, and Tsurumi T: Effect of material constants on power output in piezoelectric vibration-based generators. *IEEE Transactions on Ultrasonics, Ferroelectrics, and Frequency Control* 2011;58:1852–1859. DOI: 10.1109/TUFFC.2011.2023.
- [12] Beeby SP, Torah RN, Tudor MJ, Glynn-Jones P, O'Donnell T, Saha CR, and Roy S: A micro magnetic generator for vibration energy harvesting. *Journal of Micromechanics and Microengineering* 2007;17:1257–1265. DOI: 10.1088/0960-1317/17/7/007.
- [13] Takeuchi K. Energy Harvesting to learn from scratch *Nikkei Electronics*. 2013;12(23): 138–143.

- [14] Le TT, Han J, von Jouanne A, Mayaram K, and Fiez TS: Piezoelectric micro-power generation interface circuit. *IEEE Journal of Solid-State Circuit*. 2006;41(6):1411–1420. DOI: 10.1109/JSSC.2006.874286.
- [15] Lu C, Tsui CV, and Ki WH: Vibration energy scavenging system with maximum power tracking for micro-power applications. *IEEE Transactions on Very Large Scale Integration Systems*. 2011;19(11):2109–2119. DOI: 10.1109/TVLSI.2010.2069574.
- [16] Maiwa H and Sakamoto W: Vibrational energy harvesting using a unimorph with PZT-or BT-based ceramics. *Ferroelectrics* 2013;446(1):67–77. DOI: 10.1080/00150193.2013.821011.
- [17] Maiwa H, Sakamoto W, and Ishizone Y: Thermal and Vibrational Energy Harvesting using PZT-and BT-based ceramics. In: *Proceedings of 2012 21st IEEE Int. Symposium on Applications of Ferroelectrics held jointly with 11th IEEE European Conference on the Applications of Polar Dielectrics and IEEE PFM, (ISAF/ECAPD/PFM2012); 9–13 July 2012; Aveiro, IEEE, 6297808*. DOI: 10.1109/ISAF.2012.6297808.
- [18] NEC Tokin. *Piezoelectric Ceramics Vol05* [Internet]. 2013; Available from http://www.nec-tokin.com/english/product/pdf_dl/piezoelectricceramics.pdf [accessed: 2016-04-19].
- [19] Linear Technology. *LTC3588-1 Typical application description: nanopower energy harvesting power supply* [Internet] 2010; Available from <http://cds.linear.com/docs/en/datasheet/35881fc.pdf> [accessed: 2016-04-19].